AIAA 82-4142

Behavior of an Unsteady Turbulent Boundary Layer

P. G. Parikh,* W. C. Reynolds,† and R. Jayaraman‡
Stanford University, Stanford, Calif.

Measurements on an unsteady turbulent boundary layer with well-defined initial and boundary conditions are reported in this paper. The test boundary layer is a standard, steady, flat-plate turbulent boundary layer at the entrance to the unsteady region, and is subjected to a linearly decreasing freestream velocity in a time-dependent manner. The experiments were conducted in a specially designed water tunnel with the frequency of the imposed oscillations ranging from quasisteady ($f \to 0$) up to the "bursting frequency" in turbulent boundary layers. It was found that the mean velocity and turbulence intensity profiles were unaffected by the imposed oscillations. The amplitude ratio of the periodic component, although as much as 1.7 for quasisteady oscillations, becomes unity over the outer region of the boundary layer at higher frequencies. Both the boundary-layer thickness and the Reynolds stress distribution across the boundary layer become frozen over the oscillation cycle at high frequencies.

I. Introduction

THE term "unsteady turbulent flow" is applied to a turbulent flowfield containing a well-defined, time-dependent, organized velocity component. Unsteady turbulent boundary layers occur in a variety of engineering applications. Boundary layers on the surface of a gas turbine blade rotating in the wakes of stator vanes, on the surface of a helicopter rotor blade performing pitch oscillations, on the walls of a reciprocating engine cylinder, and in pitch oscillations, on the walls of a reciprocating engine cylinder, and in nuclear reactor components during transients are but a few examples where unsteadiness is imposed on a turbulent boundary layer.

Despite the obvious practical importance of unsteady turbulent boundary layers, very few basic experiments aimed at the development of a fundamental understanding of such flows were conducted until very recently. This was primarily due to the difficulties associated with analog processing of a velocity signal from such flows. The availability of digital signal-processing instrumentation in recent times has prompted several new experiments in the area of unsteady turbulent boundary layers.

In parallel with the development of advanced measurement and data processing techniques, great strides have been made in the art of turbulent boundary-layer prediction. Any computational scheme must, however, rely on a particular turbulence model, which is based on available data for a given flow situation. Furthermore, the validity of any prediction scheme can be checked only by comparison with available experimental data.

The objectives of the Stanford Unsteady Turbulent Boundary Layer program are to develop a fundamental understanding of such flows, to provide a definitive data base that can be used to guide turbulence-model development, and to provide a test case that can be used by computors for comparison with their prediction. In this paper, emphasis is on development of an understanding of an unsteady turbulent boundary layer subjected to a specific type of freestream unsteadiness. The experimental results are reported here in graphical form only. Digital data acquired during the present study and those being acquired in continuing studies may be found in Ref. 13.

The earliest systematic investigation of unsteady turbulent boundary layers was by Karlsson,[1] who subjected a flat-plate turbulent boundary layer to oscillation amplitudes up to 34% of the mean freestream velocity at frequencies ranging from 0 to 48 Hz. Karlsson found that imposed oscillations had practically no effect on the mean velocity profile in the boundary layer. The measurements of the amplitude and phase of the periodic component as well as of turbulence intensity were rather uncertain because of the limited accuracy of the signal-processing instruments employed.

More recently, several investigators have studied unsteady turbulent boundary layers experimentally. Patel[2] studied the behavior of a flat-plate turbulent boundary layer subjected to traveling waves in the freestream, and reported measurements of mean, periodic, and random parts of the streamwise velocity components. Kenison[3] continued the work of Patel[2] with adverse mean pressure gradient. Schachenmann and Rockwell[4] reported measurements of the boundary layer on the wall of a conical diffuser with unsteady through flow. The group of Cousteix et al. at Toulouse conducted experiments in zero as well as adverse-mean-pressure-gradient boundary layers.[5,6] In order to generate large amplitudes of imposed freestream oscillations, the latter experiments were run at a fixed frequency, which was the resonant frequency of the tunnel. Simpson[7] conducted experiments on adverse-pressure-gradient, separating, turbulent boundary layers. Unsteady boundary-layer experiments with large imposed oscillation frequencies are currently under way at Iowa Institute of Hydraulic Research (IIHR) under the direction of Ramaprian and Patel.[8] The ranges of parameters employed in these

Table 1 Ranges of experimental parameters in various investigations

Investigator	$\bar{u}_\infty$, m/s	f, Hz	$\beta_\delta = f\delta/\bar{u}_\infty$
Karlsson[1]	5	0.33-48	0.0055-0.686
Patel[2]	19.8	4-12	0.004-0.012
Kenison[3]	22	0-6	0-0.005
Schachenmann and Rockwell[4]	3	5-35	0.0072-0.058
Cousteix et al.[5]	33.6	43	0.002
Cousteix et al.[6]	30	38	0.002
Simpson[7]	22	0.6	?
Ramaprian and Patel[8]	1.0	0.1-8.0	0.005-0.38
Present	0.73	0-2.0	0-0.14

Received Jan. 14, 1981; revision received Aug. 10, 1981.

*Research Associate, Department of Mechanical Engineering; presently with Jet Propulsion Laboratory, Caltech, Pasadena, Calif.
†Professor and Chairman, Department of Mechanical Engineering.
‡Research Assistant, Department of Mechanical Engineering.

experiments will be compared with those for the present experiment in Sec. II.

All the experiments summarized above are characterized by unsteady flow at the inlet to the unsteady region. The distinctive feature of the present experiments is that the boundary layer at the inlet to the unsteady region is a standard, *steady*, flat-plate turbulent boundary layer. It is then subjected to well-defined and controlled periodic oscillations of the freestream. This feature is especially important from the point of view of a computor, who needs a rather precise specification of the initial conditions at the beginning of an unsteady computation.

II. Freestream Boundary Condition of the Present Experiment

A new water tunnel has been designed and built for the present experiments. The desired freestream velocity distribution in the tunnel is shown in Fig. 1. The freestream velocity remains *steady* and uniform for the first 2 m of boundary-layer development. It then decreases linearly in the test section such that the magnitude of the velocity *gradient* varies sinusoidally from zero to a maximum value during the oscillation cycle. The mean freestream velocity distribution in the test section is thus linearly decreasing and corresponds to the distribution at the cycle phase angle of 90 deg, while the amplitude of the imposed freestream oscillations grows linearly in the streamwise direction, starting at zero at the entrance and going to a maximum value of a_0 at the exit. Both the amplitude and the frequency of the imposed freestream oscillations may be varied in the present experiment. The freestream velocity distribution is thus governed by the equation

$$u_\infty(x,t) = u_{\infty,0} \qquad x < x_0$$

$$= u_{\infty,0} - \frac{a_0(x-x_0)}{L}[1-\cos\omega t] \qquad x_0 \le x < x_0 + L$$

The important parameters of this problem are: 1) an amplitude parameter $\alpha = a_0/u_{\infty,0}$, and 2) a frequency parameter $\beta_\delta = f\delta_0/u_{\infty,0}$ where $f = \omega/2\pi$ and δ_0 = thickness of the boundary layer at the inlet to the unsteady region. The ranges of parameters in the present experiments are as follows: $u_{\infty,0} = 0.73$ m/s, $x_0 = 2$ m, $L = 0.6$ m, $\delta_0 = 0.05$ m, $0 < f < 2$ Hz, $0 < \alpha < 0.2$, $0 < \beta_\delta < 0.14$. A comparison of the parameter range of this experiment with that of previous unsteady boundary-layer experiments is shown in Table 1.

It should be mentioned that the value of the frequency parameter β_δ at the so-called bursting frequency in turbulent boundary layers[9] is about 0.2. Thus the imposed oscillation frequencies used in the present experiments cover the range from quasisteady ($f \simeq 0$) to values approaching the bursting frequency. The results reported here are for a nondimensional amplitude $\alpha = 0.05$. An amplitude of $\alpha = 0.15$ is sufficient to cause separation of the turbulent boundary layer in the test section during a part of the oscillation cycle. Results for large-amplitude experiments including periodic separation will be presented in a future publication.

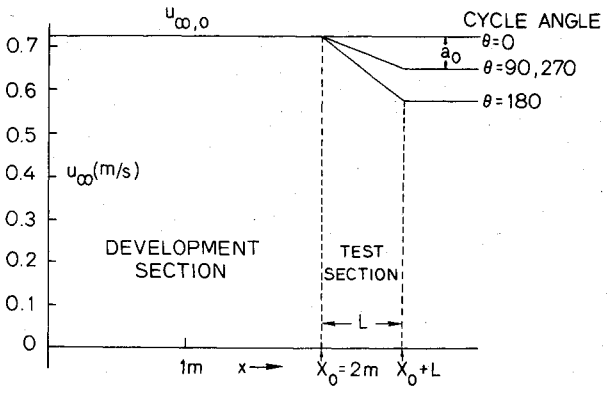

Fig. 1 Desired freestream velocity distribution.

III. Experimental Facility

A schematic of the water tunnel built for these experiments is shown in Fig. 2. The system operates at a constant head and a constant flow resistance, so that the total flow remains constant. The tunnel consists of a 16:1 nozzle contraction followed by a 2-m-long development section. The test boundary layer is grown on the top wall of the tunnel. The freestream velocity in the development section is maintained uniform along x by bleeding a small amount of flow from the bottom wall.

The linear decrease in freestream velocity in the test section is accomplished by uniform bleeding off of a fraction of the total flow through a perforated plate that forms the bottom of the test section. The remainder of the flow exits through a second perforated plate farther downstream. Flow through each perforated plate then passes on to the exit header, which contains two compartments separated by a partition plate. The flow from the two compartments exits the tunnel through a sliding-gate valve that contains a series of longitudinal slots running perpendicular to the partition plate. This design ensures that, regardless of the position of the sliding-gate valve, the total flow area of the slots remains the same. The slots are sized such that their total area constitutes the controlling resistance of the entire fluid circuit. As the sliding-gate valve is oscillated by means of a dc-motor-driven scotch yoke mechanism, the fraction of the total flow bled from the bottom wall of the test section varies in a harmonic fashion whereas the total flow through the tunnel remains constant. By this arrangement, a linearly decreasing periodic freestream distribution is established in the test section while the upstream flow (in the development section) remains steady.

IV. Measurement and Data Processing Techniques

The techniques of pitot, hot-film, and laser anemometry are employed for measurement of velocity in the present experiments. The primary technique applied to date for unsteady measurements has been a single-channel, forward-scatter DISA laser anemometer with a frequency-shift capability.

Following Hussain and Reynolds,[10] the instantaneous velocity signal from an unsteady turbulent flow may be decomposed into three parts:

$$u = \bar{u} + \tilde{u} + u' \qquad (1)$$

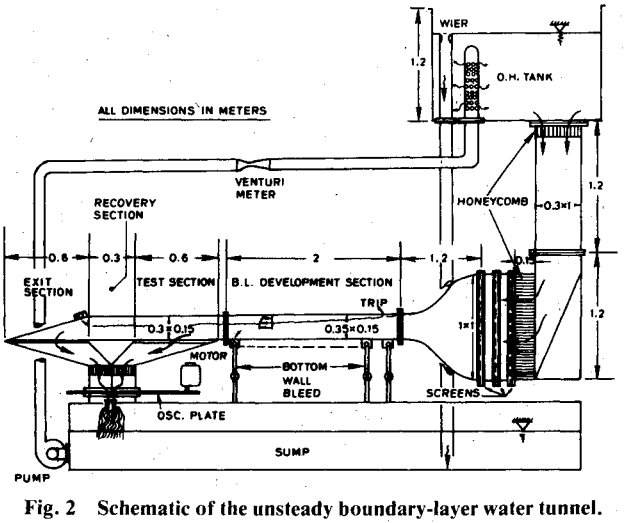

Fig. 2 Schematic of the unsteady boundary-layer water tunnel.

where $\bar{u}$ is the mean, $\tilde{u}$ is the time-dependent, organized (deterministic) component, and u' is the contribution of random fluctuations. $\bar{u}$ may be determined by a simple long-time averaging of u. In the present experiments, $\tilde{u}$ is of a periodic nature, and it may be determined by first phase averaging the instantaneous velocity signal and then subtracting out the mean. Thus,

$$\tilde{u} = \langle u \rangle - \bar{u} \tag{2}$$

where $\langle u \rangle$ is the phase average, which is determined by constructing an ensemble of samples taken at a fixed phase angle of the imposed oscillation cycle and then averaging each ensemble after a sufficient number of samples has been collected. In the present experiments, it was found that, for an imposed harmonic oscillation of the freestream (at $\alpha = 0.05$), the response at points within the boundary layer was almost sinusoidal, with a contribution of higher harmonics less than 5% of the fundamental. In view of this fact, the periodic component $\tilde{u}$ may also be extracted sufficiently accurately from the instantaneous signal u by a cross correlation with the pulser signal. The latter technique was used in obtaining the results reported here.

A digital correlator (HP 3721A) was used for determination of cross correlations. More recently, a DEC MINC-11 laboratory minicomputer system is being used for automatic data acquisition and processing that includes determination of the phase average $\langle u \rangle$.

V. Apparatus Qualification Tests

A series of qualification tests was conducted to ascertain a satisfactory operation of the tunnel as designed, and modifications were made to improve its performance. Of particular importance was the requirement of a steady upstream flow while the flow in the test section was oscillatory. Trimming adjustments to the slot area of the pulser were required to ensure that the total flow remained constant and that upstream propagation of the disturbances was acceptably small. An rms organized disturbance level of 0.3% was achieved, and this was comparable to the background freestream turbulent level in the development section.

Next, a series of boundary-layer mean velocity profiles was measured in the development section. The local momentum thickness Reynolds numbers (Re_{δ_2}) were computed from these profiles. The local skin-friction coefficient (C_f) was determined from the mean profiles by the Clauser plot technique, and the data were found to follow the correlation $C_f = 0.0128\, Re_{\delta_2}^{-1/4}$, which is accepted as a standard for a steady flat-plate turbulent boundary layer.[11] The mean velocity profile at the entrance to the unsteady region (i.e., at $x = x_0$) had $Re_{\delta_2} = 3000$ and, when plotted in velocity defect coordinates, followed Coles' law of the wake.

The measured phase-averaged, freestream velocity distribution is plotted in Fig. 3 with the cycle phase angle as the parameter. Note that the distribution is quite linear and that the organized disturbance at $x = x_0$ is quite small (rms $\simeq 0.003 u_{\infty,0}$). Digital data on initial profiles of mean velocity and turbulence intensity at the entrance to the test section as well as on phase-averaged freestream velocity distribution may be found in Ref. 13.

VI. Experimental Results

The measurements reported here were taken at a fixed streamwise location near the end of the test section at $x - x_0 = 0.57$ m. The measured mean velocity profiles at three stationary pulser positions $\theta = 0$, 90, and 180 deg are shown as dashed curves in Fig. 4a. These represent phase-averaged profiles at zero frequency, i.e., quasisteady profiles. These would indeed be the phase-averaged profiles at very low frequencies of imposed oscillations. At this value ($\alpha = 0.05$) of the amplitude of imposed oscillations, the response of the boundary layer is almost linear, so that the profile corresponding to $\theta = 90$ deg lies nearly midway between the $\theta = 0$ and 180 deg profiles, and further, the $\theta = 90$ deg profile represents the mean profile for quasisteady oscillations. Also, the difference between the $\theta = 0$ and 90 deg profiles at a fixed y location represents the amplitude of quasisteady (very-low-frequency) oscillations at that location in the boundary layer.

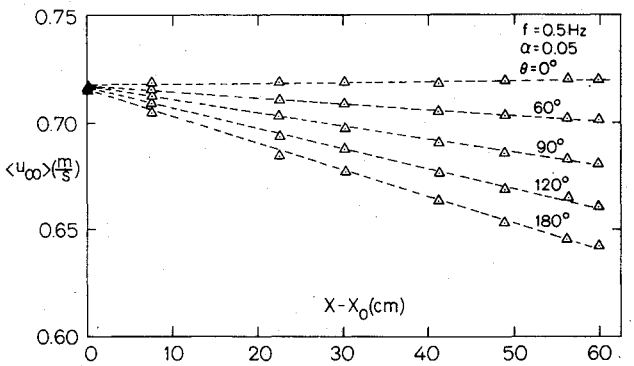

Fig. 3 Phase-averaged freestream velocity distribution.

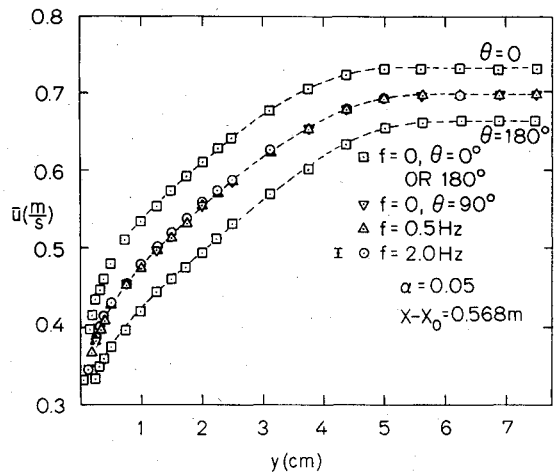

Fig. 4a Mean velocity profiles (outer region).

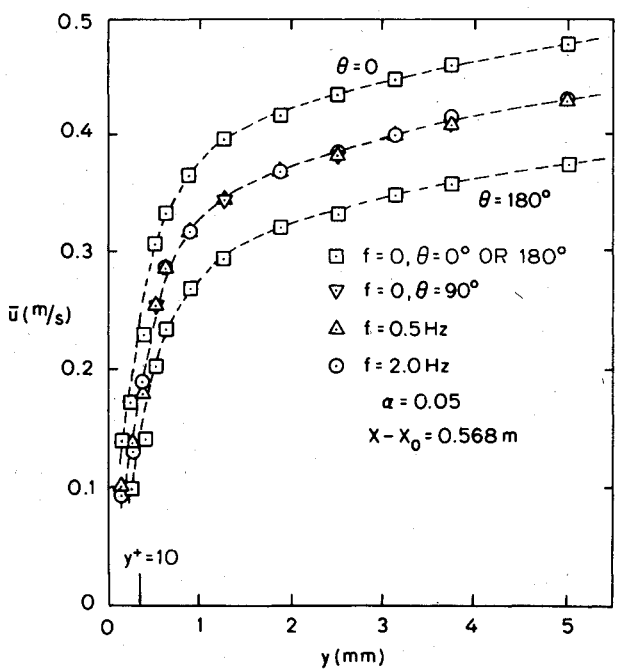

Fig. 4b Mean velocity profiles (near-wall region).

It may be seen that the quasisteady amplitudes in the boundary layer are larger than the freestream amplitude. We shall return to this point later on in the discussion.

The mean velocity profiles measured under oscillatory conditions at different frequencies are also shown in Fig. 4a. It may be seen that the mean velocity profiles at various frequencies are identical with the profile measured under stationary condition with pulser angle set at $\theta = 90$ deg. The latter profile, of course, represents the mean velocity profile for quasisteady oscillations. It may be concluded that the mean velocity profile (at a fixed amplitude $\alpha = 0.05$) is independent of the imposed oscillation frequency in the entire range $0 \leq f \leq 2$ Hz. The same behavior persists all the way up to the wall, as shown in Fig. 4b for the near-wall region.

This behavior of the mean velocity profile may be explained by an examination of the governing equations. Insertion of the three-part decomposition of the velocity field, as shown in Eq. (1), into the momentum equation of the boundary layer and subsequent time averaging yields the following equation for the mean field:

$$\bar{u}\frac{\partial \bar{u}}{\partial x} + \bar{v}\frac{\partial \bar{u}}{\partial y} = -\frac{1}{\rho}\frac{\overline{dp}}{dx} + \nu\frac{\partial^2 \bar{u}}{\partial y^2} - \frac{1}{\rho}\frac{\partial}{\partial y}[\overline{u'v'} + \overline{\tilde{u}\tilde{v}}] \quad (3)$$

Equation (3) may be recognized as the same one governing an ordinary turbulent boundary layer, except for the addition of the term $\overline{\tilde{u}\tilde{v}}$, which represents Reynolds stresses arising from the organized fluctuations in the boundary layer.

The time-mean pressure gradient $\overline{dp}/dx$ may be shown to be independent of the imposed oscillation frequency and, except for a higher-order term, is indeed the same as that obtained with the pulser stationary at the $\theta = 90$ deg position. Therefore, the mean velocity field will be frequency-dependent if and only if one or both of the following happen:

1) The distribution of Reynolds stress $\overline{u'v'}$ is altered under oscillatory conditions and is dependent on the frequency of imposed oscillations.

2) The Reynolds stress $\overline{\tilde{u}\tilde{v}}$ arising from organized fluctuations becomes significant compared with $\overline{u'v'}$.

We shall next show that neither one of the above is the case.

Figure 5 shows the measured distribution of u'_{rms} under stationary condition with the pulser at a mean position of $\theta = 90$ deg as well as those measured under oscillatory conditions at frequencies up to 2 Hz. During measurements of u'_{rms} under oscillatory conditions, the contribution of the organized fluctuations was subtracted out so that only the random part of the fluctuations is represented in Fig. 5. It may be seen that the distribution of u'_{rms} is independent of the imposed oscillation frequency and, further, that it is the same as that measured under stationary conditions with the pulser fixed at the mean position of $\theta = 90$ deg. As our present measurement system does not have the capability of measuring two components of velocity simultaneously, data on $\overline{u'v'}$ are not reported here. However, it is reasonable to assume that $\overline{u'v'}$ distribution would also remain independent of the oscillation frequency and would be the same as that measured under stationary condition at $\theta = 90$ deg.

In Fig. 6, a comparison is shown between measured values of $\overline{\tilde{u}\tilde{v}}$ at 2 Hz with data on $\overline{u'v'}$ obtained by Anderson[12] in a steady adverse-pressure-gradient boundary layer at comparable conditions. The present data on $\overline{\tilde{u}\tilde{v}}$ were obtained by separate LDA measurements of $\tilde{u}$ and $\tilde{v}$ and their respective phases. It may be seen that the contribution of $\overline{\tilde{u}\tilde{v}}$ to total Reynolds stress is insignificant over almost the entire boundary layer.

In view of the data presented in Figs. gs. 5 and 6, it is not surprising that the mean velocity profile remains independent of the imposed oscillation frequency and is indeed the same as the one measured under stationary conditions with $\theta = 90$ deg.

The behavior of the periodic component will next be examined. The profiles of amplitudes a_l measured in the boundary layer and normalized by the freestream amplitude $a_{l,\infty}$ are shown in Fig. 7. The profile for quasisteady ($f \simeq 0$) oscillations was determined, as explained earlier, from the mean velocity profiles measured under stationary conditions with the pulser set at $\theta = 0$, 90, and 180 deg (see Figs. 4a and 4b). Note that, during quasisteady oscillations, the amplitude in the boundary layer overshoots the freestream amplitude by as much as 70%. It may be mentioned that the data for $f = 0.1$ Hz, although not shown in Fig. 7, do indeed come very close to the quasisteady behavior.

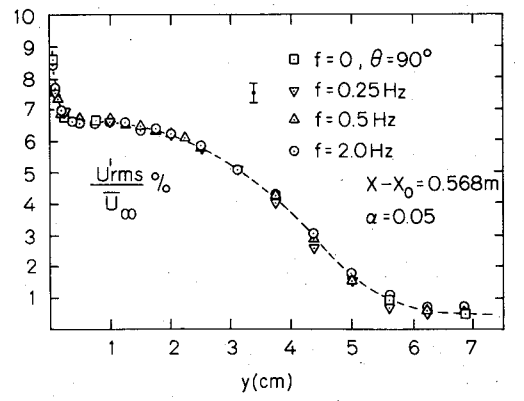

Fig. 5 Profiles of longitudinal turbulence intensity.

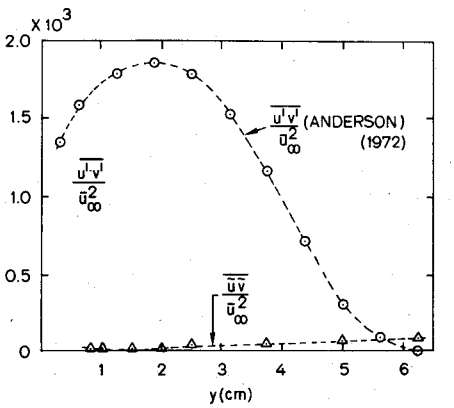

Fig. 6 Comparison of Reynolds stress of organized fluctuations with that due to random fluctuations.

The effect of dynamics is seen as the attenuation of the amplitudes within the boundary layer. Surprisingly, however, the present data show that the measured amplitudes for $f = 0.5$ are slightly below those for the $f = 2.0$ Hz case. At high frequencies of imposed oscillations, the behavior of the periodic component profile is clear: the amplitudes in most of the boundary layer are the same as the imposed freestream amplitudes. Near the wall, the amplitude of the periodic component rapidly drops to zero.

The phase differences between the boundary-layer oscillations and freestream oscillations are shown in Fig. 8. For quasisteady oscillations, obviously, there is no phase difference. The largest phase lags (of the four cases) in the outer region of the boundary layer were observed for $f = 0.25$ Hz. The effect of increasing the frequency is to reduce the phase lag in the outer region but to introduce large phase *leads* in the region very close to the wall. Clearly, the asymptotic behavior of the *outer region* for large imposed frequencies of oscillation is once again a zero phase lag with respect to freestream oscillations, as in the quasisteady case.

The combination of the asymptotic behaviors of $a_l/a_{l,\infty}$ and ϕ in the outer region for large frequencies of imposed oscillations, together with the fact that the mean velocity profile is unaffected by imposed oscillations, has the effect of freezing the boundary-layer thickness at large frequencies.

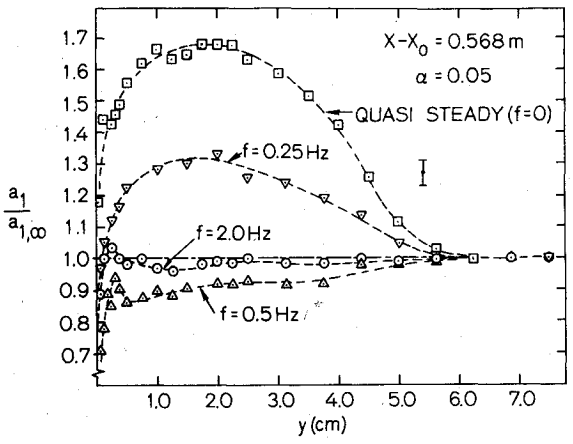

Fig. 7 Amplitude distribution across the boundary layer.

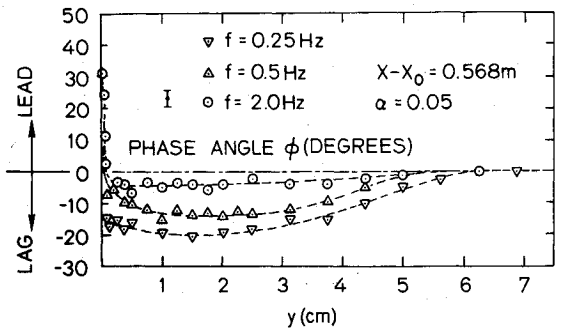

Fig. 8 Phase variation across the boundary layer.

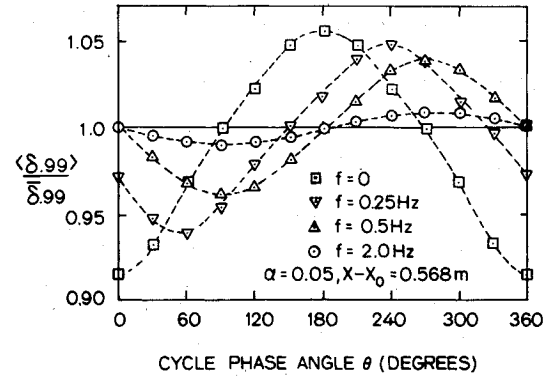

Fig. 9 Variation of instantaneous boundary-layer thickness over the oscillation cycle.

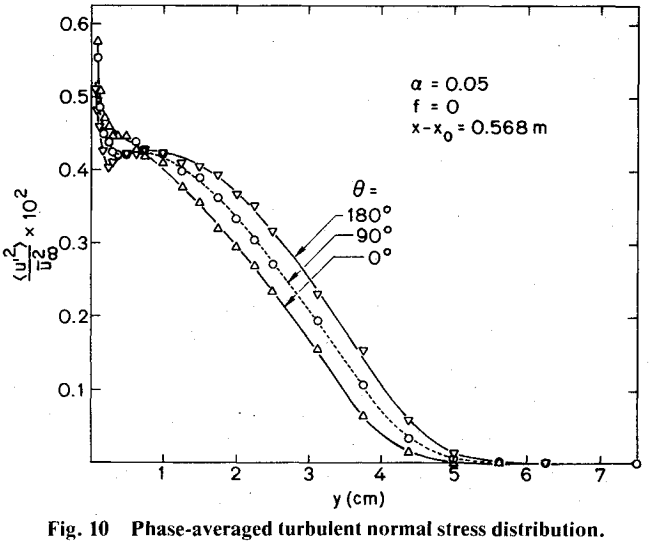

Fig. 10 Phase-averaged turbulent normal stress distribution.

This effect is shown in Fig. 9, where the instantaneous boundary-layer thickness $\langle \delta_{0.99} \rangle$, normalized by the mean boundary-layer thickness $\bar{\delta}_{0.99}$, is plotted as a function of the cycle phase angle for several frequencies of imposed oscillations. The mean boundary-layer thickness $\bar{\delta}_{0.99}$ was determined from the mean velocity profile. The quasisteady behavior of $\langle \delta_{0.99} \rangle$ is quite obvious: at $\theta = 0$, the boundary layer in the test section continues to develop under a zero pressure gradient and is the thinnest at this point in the entire cycle. As the quasisteady phase angle is increased, pressure gradients of increasing adversity are imposed on the boundary layer, causing it to thicken. The maximum thickness is attained at $\theta = 180$ deg when the magnitude of the adverse pressure gradient in the test section is at the maximum. The quasisteady boundary-layer thickness oscillates 180 deg out of phase with the freestream oscillations.

Under oscillatory conditions at $f = 0.25$, 0.5, and 2.0 Hz, two things happen: a significant phase lag develops from quasisteady behavior, and the amplitude attenuates with increasing frequency. For the $f = 2.0$ Hz case, the variation over the complete cycle is less than 1% and the boundary-layer thickness is practically frozen during the oscillation cycle.

It may be shown by a simple argument based on a mixing-length model of boundary layer turbulence that the freezing of the boundary-layer thickness at large frequencies is also accompanied by freezing of the Reynolds stress over the oscillation cycle. To prove this, we hypothesize that the phase-averaged Reynolds stress distribution may be related to the phase-averaged velocity profile in the same manner as for a steady boundary layer, i.e.,

$$-\langle u'v' \rangle = \epsilon_m \frac{\partial \langle u \rangle}{\partial y} \tag{4}$$

where

$$\epsilon_m = \ell^2 \left| \frac{\partial \langle u \rangle}{\partial y} \right| \tag{5}$$

Now, in the *outer region* of the boundary layer, the mixing length ℓ may be modeled as

$$\ell = \lambda \langle \delta_{0.99} \rangle \tag{6}$$

where λ is nearly a constant. Now,

$$\langle u \rangle = \bar{u} + \tilde{u} = \bar{u} + a_l(y) \cos[\omega t + \phi(y)] \tag{7}$$

However, in the high-frequency limit,

$$a_l(y) = a_{l,\infty} = \text{const} \qquad \phi(y) = 0 \tag{8}$$

and

$$\langle \delta_{0.99} \rangle = \bar{\delta}_{0.99} = \text{const}$$

Therefore,

$$\frac{\partial \langle u \rangle}{\partial y} = \frac{\partial \bar{u}}{\partial y} \tag{9}$$

Combining the above results,

$$\langle u'v' \rangle = -\lambda^2 (\delta_{0.99})^2 \left[\frac{\partial \bar{u}}{\partial y} \right]^2 = \overline{u'v'} \tag{10}$$

i.e., the phase-averaged Reynolds stress in the outer region also becomes frozen at a mean value $\overline{u'v'}$

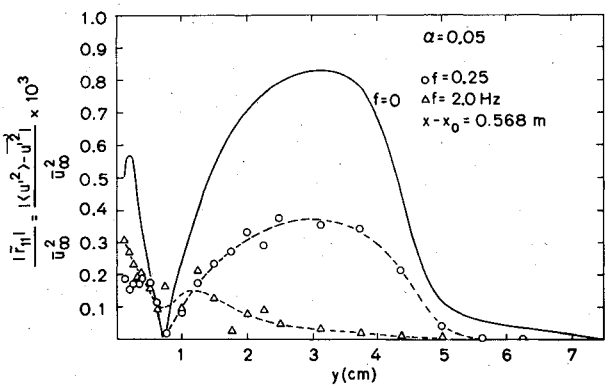

Fig. 11 Amplitude distribution of turbulent normal stress oscillations.

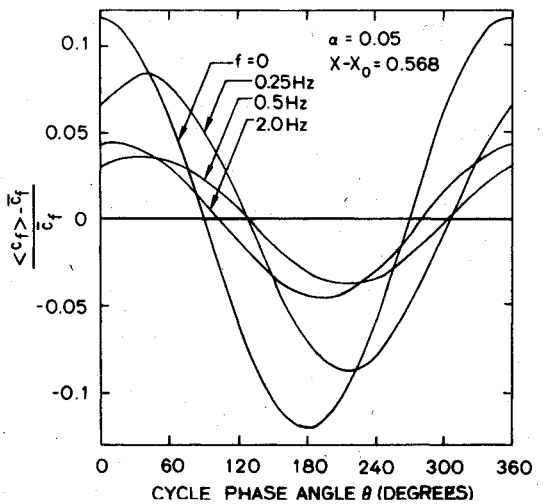

Fig. 12 Variation of skin friction over the oscillation cycle as determined by Clauser plot technique.

Experimental evidence of this stress-freezing behavior was obtained by measurements of phase-averaged normal turbulent stress $\langle u'^2 \rangle$. The quasisteady ($f=0$) profiles of $\langle u'^2 \rangle$ are shown in Fig. 10 for three phase angles, $\theta=0$, 90, and 180 deg. Note that the distribution for 90 deg lies nearly midway between those for 0 and 180 deg. The distribution of $\langle u'^2 \rangle$ for 90 deg is the same as the distribution of $\overline{u'^2}$, as seen earlier. Therefore, the difference between the 0 and 90 deg curves in Fig. 10 represents the amplitude of quasisteady oscillations of $\langle u'^2 \rangle$ at any point in the boundary layer. This amplitude was determined graphically from Fig. 10 and is plotted in Fig. 11 for the case of $f=0$. Under oscillatory conditions, the amplitude of the normal stress oscillations in the boundary layer attenuates as the frequency of imposed oscillations is increased from $f=0$. At $f=2.0$ Hz, the amplitude of stress oscillations across the boundary layer is almost zero over the outer region, as seen in Fig. 11, i.e., the stress is almost frozen over the oscillation cycle.

Finally, the variation of instantaneous skin-friction coefficient $\langle C_f \rangle$ is shown as a function of the cycle phase angle in Fig. 12. The instantaneous value of skin friction $\langle C_f \rangle$ was determined by the Clauser plot technique from the phase-averaged velocity profiles $\langle u \rangle$, assuming a law-of-the-wall equation for the log region:

$$u^+ = (1/0.41)\ell n y^+ + 5.0 \qquad (11)$$

The quasisteady variation of $\langle C_f \rangle$ is seen to be in phase with the freestream velocity oscillations, and the quasisteady amplitude is about 12% of the mean. The effect of oscillations is to introduce a phase shift and attenuate the amplitude of skin-friction variation over a cycle.

The asymptotic behavior of skin-friction variation appears to be close to the variation shown for $f=2.0$ Hz. It should be mentioned, however, that the applicability of the Clauser plot technique may be questionable in view of the large phase variations that are present in the near-wall region at high frequencies (see Fig. 8). Careful measurements in the region very close to the wall (i.e., the region between the wall and the log region) are currently under way to determine the dependence of $\bar{u}$, a_1, θ, and u' in this region on the frequency of imposed oscillations.

VII. Conclusions

The conclusions from the first phase of the present experiments (at $\alpha=0.05$) may be summarized as follows:

1) The mean velocity profile in the boundary layer is unaffected by imposed freestream oscillations in the range of frequencies employed, and it is in fact the same as the one measured with a freestream velocity distribution held steady at the mean value.

2) This behavior of the mean velocity field is a consequence of two observations: a) the time-averaged Reynolds stress distribution across the boundary layer is apparently unaffected by the imposed oscillations and is indeed the same as the one measured with the freestream velocity distribution held steady at the mean value; and b) the Reynolds stresses arising from the organized velocity fluctuations under imposed oscillatory conditions are negligible compared with the Reynolds stresses due to the random fluctuations.

3) The amplitude of the periodic component in the boundary layer under quasisteady oscillations ($f\to 0$) is as much as 70% larger than the imposed freestream amplitude. At higher frequencies of imposed oscillations, however, the peak amplitude in the boundary layer is rapidly attenuated toward an asymptotic behavior where amplitudes in the outer region of the boundary layer become the same as the freestream amplitude, dropping off to zero in the near-wall region.

4) Quasisteady boundary-layer response is in phase with the imposed oscillations. As the frequency of imposed oscillations is increased, phase lags begin to develop in the outer region of the boundary layer. The magnitude of this phase lag reaches a maximum and then decreases with increasing frequency until an asymptotic limit is reached where the outer region once again responds in phase with the freestream. Near the wall, however, large lead angles are present at higher oscillation frequencies.

5) A consequence of 3 and 4 above is that the boundary-layer thickness becomes nearly frozen over the oscillation cycle at higher frequencies.

6) A consequence of 3-5 above is that the Reynolds stress distribution in the outer region of the boundary layer also becomes frozen over the oscillation cycle at higher frequencies.

7) The skin-friction coefficient determined by the Clauser plot technique from the phase-averaged profiles under oscillatory conditions shows that the amplitude of the skin-friction oscillations at the wall appears to reach an asymptotic value at high frequencies and that this asymptotic amplitude is considerably attenuated from the quasisteady amplitude.

Acknowledgments

This research is sponsored by the Army Aeromechanics Laboratory, NASA Ames Research Center, and the Army Research Office. The authors wish to express their gratitude to Drs. Larry Carr and James McCroskey (AML), Mr. Leroy Presley (NASA Ames), and Dr. Robert Singleton (ARO) for their continued support and cooperation.

References

[1] Karlsson, S. K. F., "An Unsteady Turbulent Boundary Layer," *Journal of Fluid Mechanics*, Vol. 5, Pt. 2, May 1959, pp. 622-636.

[2]Patel, M. H., "On Turbulent Boundary Layers in Oscillatory Flow," *Proceedings of the Royal Society, Series A,* Vol. 353, 1977, pp. 121-144.

[3]Kenison, R. C., "An Experimental Study of the Effect of Oscillatory Flow on the Separation Region in a Turbulent Boundary Layer. Unsteady Aerodynamics," *AGARD Conference Proceedings No. 227,* Feb. 1978.

[4]Schachenmann, A. A. and Rockwell, D. O., "Oscillating Turbulent Flow in a Conical Diffuser," *ASME Journal of Fluid Engineering,* Dec. 1976, pp. 696-701.

[5]Cousteix, J., Desopper, A., and Houdeville, R., "Structure and Development of a Turbulent Boundary Layer in an Oscillatory External Flow," *Turbulent Shear Flows—I,* edited by F. Durst et al., Springer-Verlag, New York, 1979.

[6]Cousteix, J., Houdeville, R., and Raynaud, M., "Oscillating Turbulent Boundary Layer with a Strong Mean Pressure Gradient," presented at the 2nd Symposium on Turbulent Shear Flows, Imperial College, London, 1979.

[7]Simpson, R. L., "Features of Unsteady Turbulent Boundary Layers as Revealed from Experiments. Unsteady Aerodynamics," *AGARD Conference Proceedings No. 227,* Feb. 1978.

[8]Ramaprian, B. R. and Patel, V. C., "An Experimental Investigation of Unsteady Turbulent Boundary Layers," Iowa Institute of Hydraulic Research (IIHR), University of Iowa, private communication, 1980.

[9]Rao, K. N. et al., "The 'Bursting Phenomenon' in a Turbulent Boundary Layer," *Journal of Fluid Mechanics,* Vol. 48, Pt. 2, 1971, pp. 339-352.

[10]Hussain, A. K. M. F. and Reynolds, W. C., "The Mechanics of an Organized Wave in Turbulent Shear Flow," *Journal of Fluid Mechanics,* Pts. I, II, and III, Vol. 41, 1970, pp. 241-258, and Vol. 54, 1972, pp. 241-288.

[11]Kays, W. M. and Moffat, R. J., "The Behavior of Transpired Turbulent Boundary Layers," Dept. of Mechanical Engineering, Stanford Univ., Rept. HMT-20, 1975.

[12]Andersen, P. S., Kays, W. M., and Moffat, R. J., "The Turbulent Boundary Layer on a Porous Plate: An Experimental Study of the Fluid Mechanics for Adverse Free-Stream Pressure Gradients," Dept. of Mechanical Engineering, Stanford Univ., Rept. HMT-15, 1972.

[13]Carr, L. W., "A Compilation of Existing Unsteady Turbulent Boundary Layer Experimental Data," AGARDograph AG-265, 1981.